



## OPEN Fermented seaweed extracts ameliorate diabetic nephropathy in streptozotocin-induced diabetic rats via PI3K/AKT/mTOR pathway

Mengrui Cai<sup>1,5</sup>, Guangjian Hou<sup>3,4,5</sup>, Shousen Guo<sup>1</sup>, Yongxuan Liu<sup>1</sup>, Chen Zhao<sup>1</sup>, Lin Zhao<sup>1</sup>, Le Su<sup>1</sup>, Kunlun Li<sup>3</sup>, Qiulin Yue<sup>1,2</sup>✉ & Song Zhang<sup>1</sup>✉

The seaweed *Laminaria japonica* possesses a wide range of nutritional and medicinal properties, such as antioxidant and hypoglycemic effects. Previous research has demonstrated that fermenting *Laminaria japonica* with *S. cerevisiae* and *Lactobacillus* enhances its bioactivities. In this study, fermented *Laminaria japonica* underwent ethanol extraction to recover bioactive compounds. The impact of fermented seaweed extracts (FSE) on renal injury in streptozotocin-induced diabetic nephropathy rats was examined. Through UHPLC-MS/MS analysis, 44 compounds were identified in the fermented seaweed extracts, with carbohydrates and organic acids being the main classes. Fermented seaweed extracts significantly reduced streptozotocin-induced hyperglycemia, improved renal function markers (BUN, SCr, and Umalb), and mitigated kidney morphological changes. Specifically, the FSE-H group exhibited a 49% reduction in fasting glucose levels compared to the model group. Additionally, fermented seaweed extracts treatment downregulated both the transcriptional and protein levels of PI3K, Akt, and mTOR, suggesting involvement of the PI3K/AKT/mTOR-regulated pathway. These findings suggest that fermented seaweed extracts have potential as a therapeutic agent or functional ingredient for the treatment of diabetic nephropathy.

**Keywords** *Laminaria japonica*, Fermentation, Diabetic nephropathy, PI3K/Akt/mTOR

### Abbreviations

FSE	Fermented seaweed extracts
NC	Normal control
DN	Diabetic nephropathy group
CAP	Captopril group
FSE-H	High-dose FSE treatment group
FSE-L	Low-dose FSE treatment group
HOMA-IR	Homeostatic model assessment of insulin resistance
STZ	Streptozotocin
HE	Hematoxylin eosin
PAS	Periodic acid-schiff
KI	Kidney index
PI3K	Phosphatidylinositol-3-kinase
Akt	RAC-alpha serine/threonine-protein kinase
mTOR	mammalian target of rapamycin
GLU	Glucose
BUN	Blood urea nitrogen
SCr	Serum creatinine
Umalb	Urinary microalbumin

<sup>1</sup>State Key Laboratory of Biobased Material and Green Papermaking, Shandong Provincial Key Laboratory of Microbial Engineering, Qilu University of Technology (Shandong Academy of Sciences), Jinan 250353, P.R. China.

<sup>2</sup>Shandong Xiaoying Biotechnology Co., Ltd., Jinan 250003, China. <sup>3</sup>Jinan Hangchen Biotechnology Co., Ltd., Jinan 250002, China. <sup>4</sup>The First Clinical Medical College, Shandong University of Traditional Chinese Medicine, Jinan 250355, China. <sup>5</sup>Mengrui Caia and Guangjian Hou contributed equally to this work. ✉email: yueqiulin88@163.com; zhangsrz@163.com

The incidence of diabetic nephropathy (DN) has rapidly increased in the last decade, affecting approximately 25–40% of patients with diabetes and now representing almost 50% of all end-stage renal disease cases<sup>1</sup>. The pathogenesis of DN is multifaceted, involving hyperglycemia-mediated intracellular metabolic disturbances, autophagy, oxidative stress, and endoplasmic reticulum stress, resulting in increased tethered matrix, basement membrane thickening, and persistent proteinuria<sup>2,3</sup>. Clinical treatment for diabetic nephropathy (DN) typically involves angiotensin-converting enzyme inhibitors and angiotensin receptor blockers<sup>4</sup> although these medications can lead to adverse effects like hyperkalemia, dry cough, and angioedema<sup>5</sup>. While the underlying mechanisms of diabetic nephropathy remain unidentified, clinical studies have demonstrated that tight glycemic control can effectively delay its progression<sup>6</sup>. The PI3K/AKT/mTOR pathway is a critical signaling cascade that regulates various cellular processes, including cell growth, survival, metabolism, and autophagy<sup>7</sup>. Inhibition of the PI3K/AKT/mTOR pathway has been shown to restore autophagy, reduce oxidative stress, and ameliorate renal injury in diabetic nephropathy<sup>8</sup>. Natural compounds have demonstrated potential in modulating this pathway, making them promising candidates for the treatment of DN.

Seaweeds, a valuable marine resource traditionally used for food, feed, and medicine, contain active compounds such as polysaccharides, fucoxanthin, astaxanthin, and flavonoids. These components exhibit various biological activities including hypoglycemic, hypolipidemic, and anti-inflammatory properties<sup>9</sup>. Research indicates that seaweed consumption may positively influence risk markers associated with type 2 diabetes (T2D) and its progression. For example, a study involving dried Nordic seaweed species demonstrated significant improvements in glycemic control and lipid levels in diabetic mice, suggesting that these seaweeds could be effective in managing diabetes-related conditions<sup>10</sup>. Additionally, the incorporation of seaweed extracts in dietary interventions has been linked to lower postprandial blood glucose levels in prediabetic individuals, indicating their potential role in glycemic management<sup>11</sup>. Moreover, the prebiotic potential of seaweed-derived polysaccharides can enhance gut health, which is increasingly recognized as a factor in metabolic health. The fermentation of these polysaccharides by gut microbiota can lead to the production of short-chain fatty acids (SCFAs), which have been associated with improved insulin sensitivity and reduced inflammation, both of which are beneficial for managing glycemic levels<sup>12</sup>.

Fermentation of food materials by appropriate microorganisms can lead to the production of novel actives and an increase in biologically active compounds, ultimately enhancing bioactivity<sup>13</sup>. Our previous study demonstrated that the enhanced hypoglycemic activity of fermented *Laminaria japonica* was a result of metabolite changes due to microbial metabolism, as well as the interactive effects of these altered metabolites<sup>14</sup>. Accumulation of oligosaccharides, organic acids, phenolics, and unsaturated fatty acids was detected in the fermented *L. japonica* compared to the non-fermented extracts. Currently, there is limited research on the structure and bioactive properties of biotransformed seaweed, particularly concerning their therapeutic effects on DN. Consequently, there is a growing need to investigate the composition and efficacy of these bioactive compounds for potential use as safe alternatives in the biomedical and food industries.

The study aimed to extract bioactive compounds from *L. japonica* post-fermentation with *S. cerevisiae* and *Lactobacillus*. Ultraperformance liquid chromatography-mass spectrometry was used to analyze the bioactive fractions of the fermented seaweed extracts. The impact of these extracts on diabetic nephropathy in streptozotocin-induced diabetic rats was assessed in vivo.

## Results

### Compositional analysis of fermented seaweed extracts

The yield of fermented seaweed extract was 39.2%, calculated based on the weight ratio of dried seaweed. As illustrated in Table 1, the analysis revealed that the fermented seaweed extract contained the following components: ash (15.16% ± 0.024%), carbohydrates (45.59% ± 0.03%), protein (0.23% ± 0.001%), titratable acidity (20.71% ± 0.004%), soluble dietary fiber (7.59% ± 0.001%), total phenolics (3.40% ± 0.001%), free amino acids (5.70% ± 0.001%), and fat (0.92% ± 0.002%). The fermented seaweed extracts samples were analysed by UHPLC-MS/MS to identify their chemical composition. Utilizing data such as retention time, accurate mass-to-charge ratio, and secondary fragment ion information, a mass bank search was conducted to identify and screen the target compounds. In total, 44 compounds were identified and categorized into five groups: 21 carbohydrates, 10 organic acids, 4 amino acids, 6 polyphenols, and various vitamins. Carbohydrates were found to be the most abundant components, followed by organic acids (Table 2).

Component (%)	FSE
Ash	15.16 ± 0.024
Carbohydrate	45.59 ± 0.03
Protein	0.23 ± 0.001
Titratable acidity	20.71 ± 0.004
Soluble dietary fiber	7.59 ± 0.001
Total phenolic	3.40 ± 0.001
Fat	0.92 ± 0.002
Free amino acids	5.70 ± 0.001

**Table 1.** Chemical composition of the main nutrients in FSE.

No.	Sort	RT (min)	Observed m/z	MS/MS	Compounds	Molecular Formula
1	Carbohydrate	4.2	371	125 197 241 311	3-Man2GlcNAc	C20H35NO16
2		4.5	533	109 201 327 371	3-Man4GlcNAc	C32H55NO26
3		5	1423	254 332 415 644	GalGlcNAcMan3GlcNAc2-I	C48H81N3O36
4		5.6	533	270 391 533 765	3-Man3GlcNAc	C26H45NO21
5		5.9	371	117 244 358 674	4-GlcNAc3Man3GlcNAc2	C58H97N5O41
6		10.4	883	103 211 264 397	ManGlcNAcFucGlcNAc	C28H48N2O20
7		11.3	692	177 245 430 435	Man3GlcNAcFucGlcNAc	C40H68N2O30
8		12.7	1245	114 209 435 566	GalGlcNAc2Man2GlcNAcManGlcNAcFucGlcNAc-II	C70H117N5O50
9		12.9	1044	157 255 283 537	Gal2GlcNAc2Man3GlcNAcFucGlcNAc	C68H114N4O50
10		13.8	858	115 273 428 603	Man4GlcNAc-II	C32H55NO26
11		15.3	736	133 206 265 558	4-GlcNAc3Man3GlcNAc2	C58H97N5O41
12		16.2	755	175 265 489 521	GalNAc2FucGlcNAcGA	C32H53N3O21
13		16.4	371	175 265	6-Man4GlcNAc-II	C32H55NO26
14		17	1102	106 297 393 410	GlcNAc2Man2GlcNAcManGlcNAcFucGlcNAc	C64H107N5O45
15		17.6	696	264 364 572 646	Man5GlcNAc-I	C38H65NO31
16		18.3	998	387 429 572 739	GalGlcNAc2Man2GlcNAcManGlcNAcFucGlcNAc-II	C70H117N5O50
17		18.5	660	157 517 621 660	FucGlcNAcThrNAc	C20H34N2O13
18		19.6	674	117 175 487 767	Man2GlcNAcFucGlcNAc	C34H58N2O25
19		20.6	586	101 334 715 864	ManGlcNAc2	C22H38N2O16
20		20.8	732	184 285 468 781	4-GlcNAc3Man3GlcNAc2	C58H97N5O41
21		21.6	1054	104 184 311 494	GalGlcNAc2Man3GlcNAcFucGlcNAc-II	C62H104N4O45
22	Organic acids	4.3	134	85 108 131	L-(-)-Malic acid	C4H6O5
23		6.2	303	125 195 120 254	Arachidonic acid	C20H32O2
24		7.2	231	127 144 178 217	4-(2,4-Dichlorophenoxy)butanoic acid	C10H10Cl2O3
25		7.4	181	105 146 158 180	Linoleic acid	C18H32O2
26		7.7	156	84 158 147 120	Pantothenic acid	C9H17NO5
27		13.2	481	100 183 115 213	2-Oxoglutaric acid	C5H6O5
28		18.9	737	163 183 267 327	Dehydroeburicoic acid	C31H48O3
29		19.3	276	89 100 116 167	Eicosapentaenoic acid	C20H30O2
30		19.8	369	89 116 177 241	Digalacturonic acid	C12H18O13
31		20.2	339	163 183 255 279	Carminic acid	C22H20O13
32	Amino acid	5.3	131	117 119 129	4-Hydroxy-L-proline	C5H9NO3
33		8.5	173	125 159 146 173	N-Acetyl-L-Leucine	C8H15NO3
34		10.4	204	103 211 264 273	L-Tryptophan	C11H12N2O2
35		14.2	749	116 152 255 311	Taurine	C2H7NO3S
36	Polyphenols	7.7	898	84 120 180 337	[Gallocatechin-(4 $\alpha$ ->8)]2-catechin	C45H38O20
37		9.6	351	206 263 309 415	Artocaprin	C26H28O6
38		12.1	287	117 120 177 265	Cyanidin	[C15H11O6] <sup>+</sup>
39		13.5	571	257 209 322 367	Luteolin	C15H10O6
40		15.4	339	96 152 196 221	Secoisolaricresinol diglucoside	C20H25N3O2
41	17.1	682	89 171 189 297	Cirsiliol	C42H83NO5	
42	Vitamins	8	442	112 158 160 231	Folic acid	C19H19N7O6
43		14.7	442	117 206 283 309	Vitamin Be	
44		15.8	265	175 265	Thiamine	

**Table 2.** Information of the compounds identified in the fermented seaweed extracts by UHPLC-MS/MS.

### Effect of fermented seaweed extracts on biochemical parameters in STZ-induced diabetic rats

After 1 week of adaptive feeding, STZ (50 mg/kg) was injected intraperitoneally to establish the DN model (Fig. 1). Following injection of streptozotocin, all experimental groups exhibited growth retardation, with no significant differences observed among the model group and the other groups (Fig. 2A). At week 14, fasting glucose concentrations showed a significant difference between the diabetic nephropathy model group of rats and the normal control group of rats ( $P < 0.001$ ). The fasting glucose level in the FSE-H group was 13.9 mmol/L, representing a 49% decrease compared to the model group, as depicted in Fig. 2B. From week 0 to week 14, the fasting blood glucose levels decreased by 40.85% and 27.96% in the FSE-H and FSE-L groups, respectively, before and after treatment. In contrast, the fasting blood glucose levels in the captopril and DN groups increased by week 14. No significant difference in fasting blood glucose levels was observed between captopril-treated

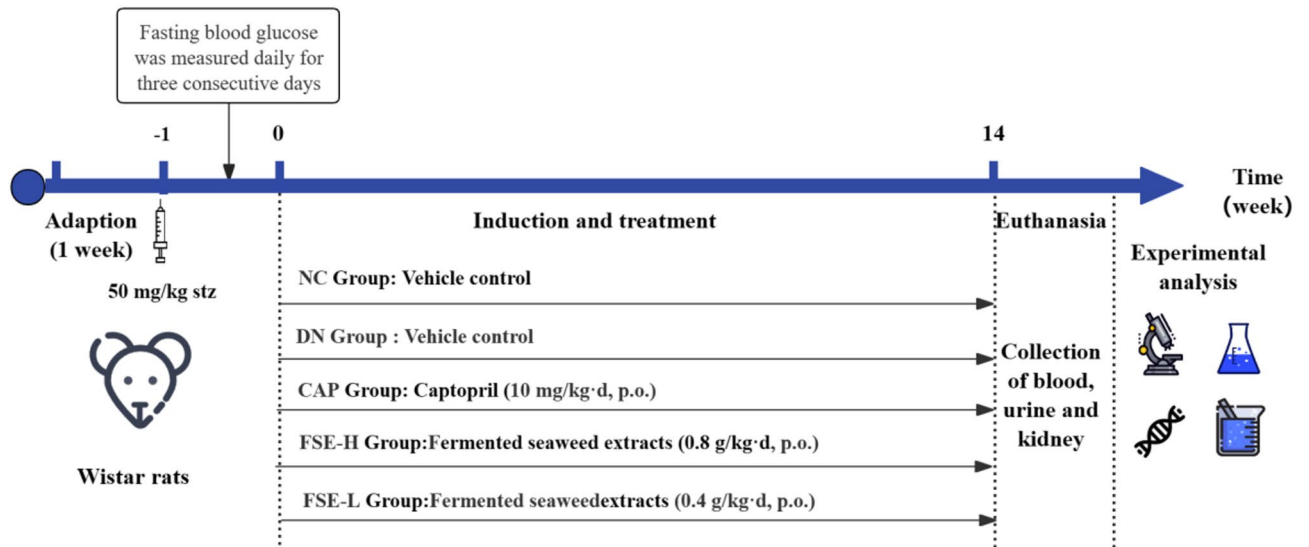


**Fig. 1.** Timeline of animal experiments. After 1 week of adaptive feeding, STZ (50 mg/kg) was injected intraperitoneally to establish the DN model. Diabetic rats were randomly divided into model group (DN), positive control group (captopril 10 mg/kg) and two groups (FSE 0.4, 0.8 g/kg). After 14 weeks of dosing, serum and urine were collected to measure renal function. NC, Normal Control; DN, Diabetic Nephropathy group; CAP, Captopril group; FSE-H, High-dose FSE treatment group; FSE-L, Low-dose FSE treatment group.

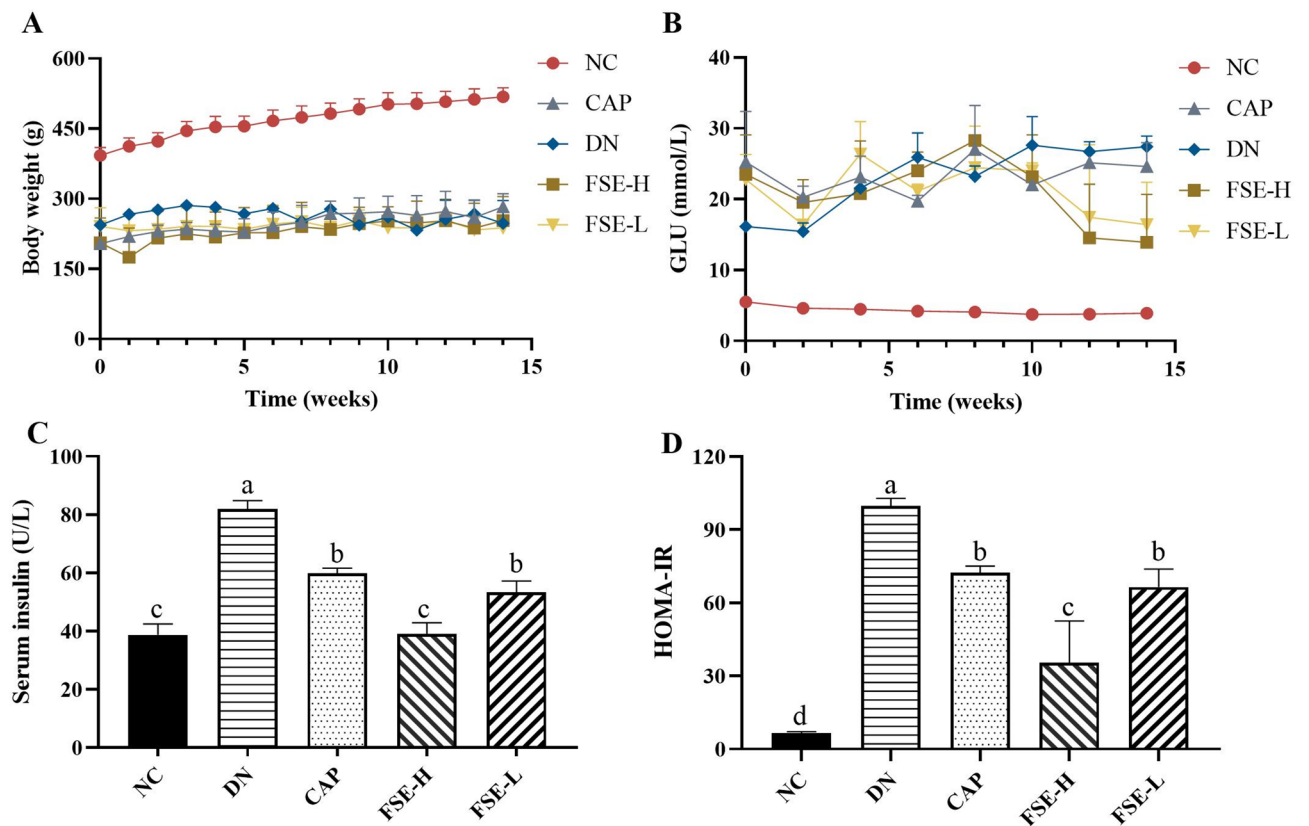


**Fig. 2.** Effects of FSE on glucose metabolism and body weight in STZ-induced diabetic rats. (A) Body weight. (B) Fasting glucose levels at weeks 0, 2, 4, 6, 8, 10, 12 and 14. (C) Serum insulin and (D) HOMA-IR changes for each group at the end of this experiment. Data are presented as mean  $\pm$  SD ( $n = 6$ ). Different letters represent significant differences among treatments when  $p < 0.05$ . NC, Normal Control; DN, Diabetic Nephropathy group; CAP, Captopril group; FSE-H, High-dose FSE treatment group; FSE-L, Low-dose FSE treatment group.

diabetic rats and model group rats. The FSE groups demonstrated a notable hypoglycemic effect in a dose-dependent manner (Fig. 2B). Furthermore, fermented seaweed extracts significantly reduced serum insulin level and HOMA-IR in DN rats ( $p < 0.001$ ) (Figs. 2C, D).

### Effect of fermented seaweed extracts on renal function in STZ-induced diabetic rats

The increased urine volume is a hallmark of diabetic nephropathy, resulting from hyperglycemia-induced osmotic diuresis and impaired renal reabsorption. Additionally, the renal functions of 24-hour urine proteins, BUN, and Scr were assessed in this study. Results showed significantly higher levels of these biomarkers in DN rats compared to normal control rats (Fig. 3). However, after 14 weeks of treatment with FSE (0.4–0.8 g/kg), the levels of these biomarkers decreased in the DN rats. Interestingly, there was no significant difference between

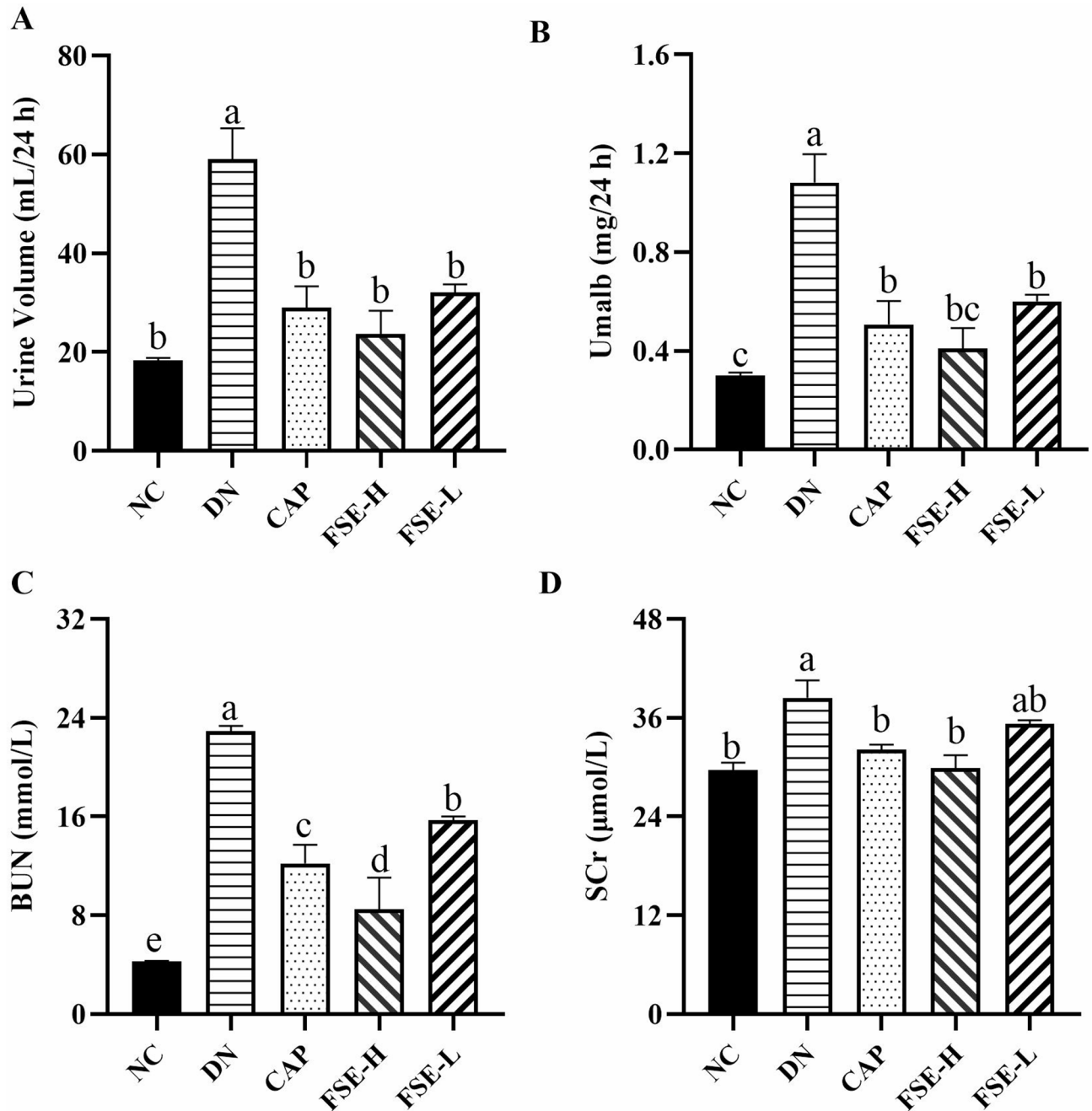


**Fig. 3.** FSE ameliorated renal injury in STZ-induced diabetic rats. (A) 24-hour urine volume. (B) Quantification of 24-hour urinary microalbumin. (C) Blood urea nitrogen levels in rats in each group after treatment. (D) Serum creatinine levels in each group at week 14. Data are presented as mean  $\pm$  SD ( $n = 6$ ). Different letters represent significant differences among treatments when  $p < 0.05$ . NC, Normal Control; DN, Diabetic Nephropathy group; CAP, Captopril group; FSE-H, High-dose FSE treatment group; FSE-L, Low-dose FSE treatment group.

the effects of FSE-H and CAP treatments. These findings collectively demonstrate the strong protective effects of fermented seaweed extracts on diabetic rats with renal injury.

### Fermented seaweed extracts ameliorated renal pathological changes in STZ-induced diabetic rats

As shown in Fig. 4B, in comparison to the normal control rats, the rats in the diabetic nephropathy group exhibited markedly elevated renal indices. Treatment with fermented seaweed extract and captopril effectively mitigated renal hypertrophy. The study evaluated morphological changes in the kidneys through sectioning for HE and PAS staining (Figs. 4A, C-D). In the normal control group, renal morphology appeared normal, with intact renal tubules and glomeruli showing no obvious pathological changes. In contrast, the diabetic nephropathy group exhibited accumulation of extracellular matrix (ECM), lobular changes in glomeruli, and thickening of the basement membrane. Following treatment with fermented seaweed extracts and captopril, these pathological impairments showed significant improvement.

### Fermented seaweed extracts exert renoprotective effects by inhibiting the PI3K/Akt/mTOR signaling pathway

Expression levels of PI3K, Akt, and mTOR genes in rat kidneys were analyzed in this study. RT-PCR results demonstrated a significant increase in mRNA levels of PI3K, Akt, and mTOR in renal tissues of the diabetic

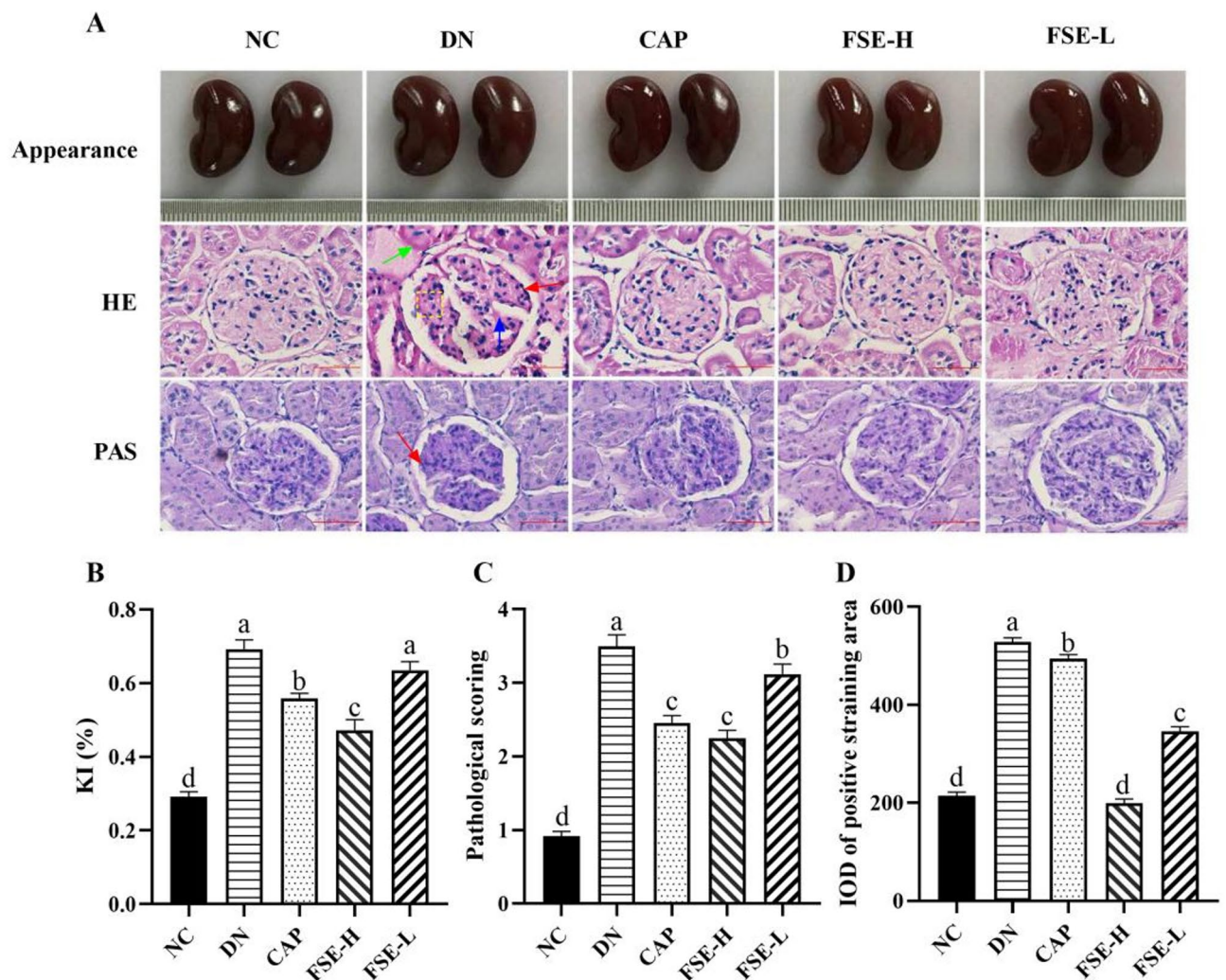


**Fig. 4.** FSE restores histological changes in the kidneys of DN rats. (A) Renal appearance, HE staining and periodic acid Schiff staining of renals in each group after treatment (original magnification,  $\times 400$ ). Green arrow indicates tubular basement membrane thickening, red arrows indicate glomerular basement membrane thickening, yellow marker indicates extracellular matrix (ECM) accumulation, and blue arrow indicates glomerular lobular change. (B) Rat kidney index (KI) in each group. (C) Pathological score of renal injury. (D) The relative IOD of PAS staining. Different letters represent significant differences among treatments when  $p < 0.05$ . NC, Normal Control; DN, Diabetic Nephropathy group; CAP, Captopril group; FSE-H, High-dose FSE treatment group; FSE-L, Low-dose FSE treatment group.

nephropathy model group compared to the NC group (Fig. 5A–C). After treatment with a high dose of fermented seaweed extracts, a notable decrease in mRNA levels of PI3K, Akt, and mTOR was observed in comparison to the model group. This indicates that fermented seaweed extracts effectively reduces the expression of PI3K/Akt/mTOR pathway-related genes in diabetic nephropathy rats. Interestingly, no significant differences were found between the CAP group and DN group, suggesting involvement of a distinct action pathway.

To further investigate the renoprotective mechanisms of fermented seaweed extracts, we analyzed the expression levels of proteins within the PI3K/Akt/mTOR signaling pathway in kidney tissues. The western blot results indicated that the phosphorylated PI3K protein content in the DN group was higher than that in the NC group, while the protein content in the FSE-H group was significantly lower than in the other groups (Fig. 5E). In the DN group, the phosphorylated protein levels of Akt and mTOR were significantly elevated (Fig. 5F, G). After treatment with FSE, the phosphorylations of Akt and mTOR were markedly reduced, compared to the model group. These findings suggest that fermented seaweed extracts confer protection to kidney function by inhibiting the PI3K/Akt/mTOR signaling pathway.

## Discussion

Diabetic nephropathy, a significant microvascular complication of diabetes mellitus, is a leading cause of chronic kidney disease and end-stage renal disease<sup>15,16</sup>. Current treatment strategies for diabetic nephropathy focus on controlling blood glucose, blood lipids, and blood pressure<sup>17</sup>. Recently, there has been growing interest in natural compounds as valuable therapeutic options. Our previous research demonstrated that fermented seaweed extracts, produced through fermentation with *S. cerevisiae* and *L. plantarum*, exhibited stronger hypoglycemic effects compared to unfermented seaweeds<sup>14</sup>. *S. cerevisiae* primarily degrades complex carbohydrates into simpler sugars, while *L. plantarum* further metabolizes these sugars into organic acids and other bioactive compounds. This synergistic process maximizes the bioactivity of the final extract. Fermentation is a specialized process that can alter the properties of raw materials, with many fermented products showing promise in treating early diabetic nephropathy. Studies have also highlighted the potential benefits of fermented red bean extract and fermented astragalus in alleviating diabetic nephropathy<sup>18,19</sup>. In our investigation, we explored the impact of fermented seaweed extracts on diabetic nephropathy in streptozotocin-induced diabetic rats.

The results indicated that fermented seaweed extracts improved insulin resistance in a dose-dependent manner. Insulin resistance, a condition where cells or tissues exhibit reduced responsiveness to insulin, was quantitatively assessed using HOMA-IR<sup>20</sup>. The findings suggest that fermented seaweed extracts effectively mitigate insulin resistance and enhance cellular sensitivity to insulin in diabetic nephropathy rats. Biochemical indicators such as SCr, BUN, and Umalb are commonly used to monitor renal function progression<sup>21</sup>. As renal fibrosis advances, there is a decrease in renal filtration leading to the accumulation of metabolic wastes like SCr and BUN in the blood. Numerous studies have linked changes in these markers with the development of DN<sup>22,23</sup>. Therefore, in this study, we tracked SCr, BUN, and Umalb levels in rats. The results indicated that DN rats displayed typical renal dysfunction, with elevated SCr, BUN, and Umalb levels. Treatment with FSE notably reduced these values, suggesting a protective effect against renal insufficiency in DN rats. Through histological

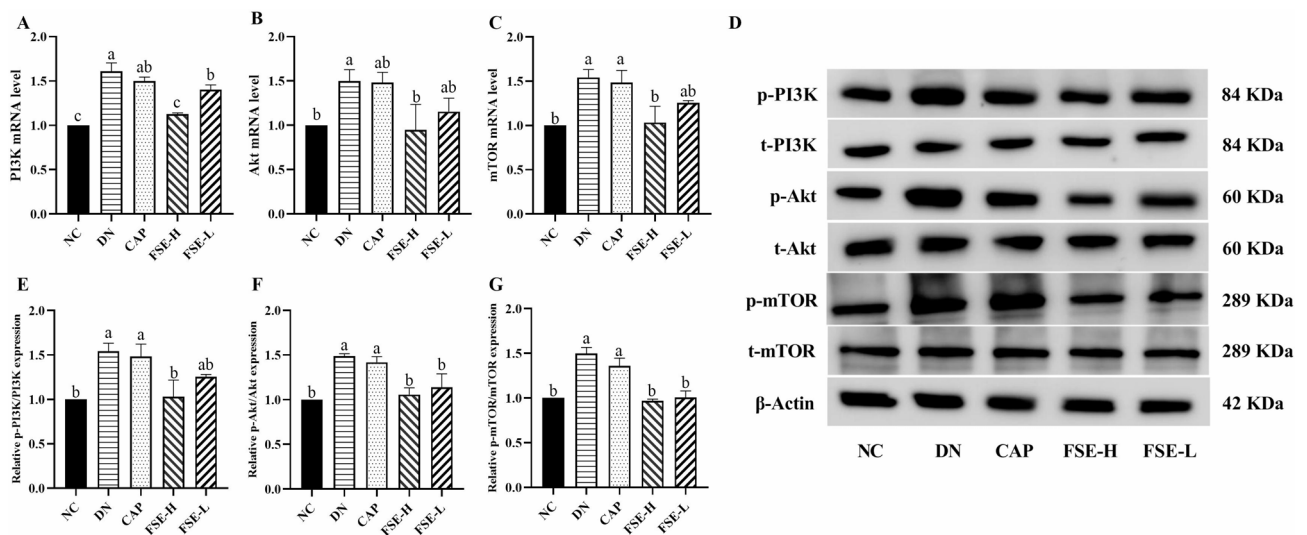


**Fig. 5.** FSE inhibits the PI3K/AKT/mTOR signaling pathway in diabetic rats. The mRNA expression levels of PI3K (A), Akt (B), and mTOR (C) in different groups of rats. The results of western blot assays for phosphorylated PI3K (P-PI3K), total PI3K, phosphorylated AKT (P-AKT), total AKT, phosphorylated mTOR (P-mTOR), and total mTOR protein expression in the kidneys of rats (D) and quantification of the ratios of P-PI3K to PI3K (E), P-AKT to AKT (F), and P-mTOR to mTOR (G).  $\beta$ -Actin was used as an internal control. Data are presented as mean  $\pm$  SD ( $n = 6$ ). Different letters represent significant differences among treatments when  $p < 0.05$ . NC, Normal Control; DN, Diabetic Nephropathy group; CAP, Captopril group; FSE-H, High-dose FSE treatment group; FSE-L, Low-dose FSE treatment group.

examination using HE and PAS staining, we found that FSE significantly mitigated renal histopathological lesions and notably reduced glycogen hyperaccumulation in DN rats. Collectively, these findings provide compelling evidence for the nephroprotective effects of FSE on the kidneys of DN rats.

Bioactive compounds, such as oligosaccharides, organic acids, and polyphenols, were found to increase in seaweed after fermentation with probiotics. Several research studies have shown that seaweed carbohydrates possess various bioactivities, including hypoglycemic and antioxidant properties<sup>24–26</sup>. Recent research has suggested that lower molecular weight carbohydrates exhibit superior hypoglycemic activity compared to larger molecules<sup>27,28</sup>. In this study, oligosaccharides were identified as the predominant components in the fermented seaweed extracts, potentially contributing to the observed hypoglycemic effects which could help in alleviating diabetic nephropathy. Furthermore, L-malic acid, butyric acid, and arachidonic acid recognized for their capacity to lower blood glucose levels and demonstrate antidiabetic effects<sup>29–31</sup> were also identified in the fermented seaweed extracts. Their concentrations were found to be higher than those in the unfermented analogues, suggesting that they may serve as prebiotic compounds generated during the fermentation process.

Studies have indicated that both organic acids and oligosaccharides can improve hyperglycemia by restoring the normal function of pancreatic islet cells<sup>20,32</sup>. Numerous studies have demonstrated that carbohydrates derived from seaweed exhibit a variety of bioactivities, including hypoglycemic and antioxidant effects<sup>24–26</sup>. Recent research indicates that lower molecular weight carbohydrates display superior hypoglycemic activity compared to their larger counterparts<sup>27,28</sup>. Furthermore, alginate oligosaccharides extracted from seaweeds have been shown to significantly reduce oxidative stress in mouse kidneys and substantially improve pathological changes within these organs<sup>33</sup>. In this study, oligosaccharides were identified as the predominant components in the fermented seaweed extracts, potentially contributing to the observed hypoglycemic effects that may aid in alleviating diabetic nephropathy. However, there is a notable absence of studies examining the oligosaccharides found in fermented seaweed extracts for the treatment of nephropathy. Butyric acid ameliorates diabetic nephropathy by inhibiting oxidative stress and activating NF- $\kappa$ B signals<sup>34</sup>. The protective effects of luteolin against diabetic nephropathy have also been documented<sup>35</sup>. It attenuates renal fibrosis in diabetic nephropathy by modulating the AMPK/NLRP3/TGF- $\beta$  signalling pathway to reduce energy metabolism disorders and inflammatory responses<sup>36</sup>. The potential alleviation of diabetic nephropathy by fermented seaweed extracts may be attributed to the synergistic and additive effects of the bioactive compounds present.

The PI3K/AKT/mTOR signaling pathway is known to play a crucial role in the development of DN. This pathway is primarily regulated by nutrients and energy through the upstream phosphatidylinositol 3-kinase/protein kinase B (PI3K/Akt) signaling pathway<sup>31</sup>. Trophic factors can activate PI3K via receptor tyrosine kinases, leading to the phosphorylation of Akt and subsequent regulation of mTOR activity<sup>7</sup>. The PI3K/AKT/mTOR signaling pathway regulates multiple pathways in diabetic nephropathy, influencing various aspects of cell growth, survival, metabolism, and inflammatory responses<sup>8</sup>. Activation of this pathway may result in excessive cell proliferation and survival, accumulation of metabolites in the kidney, promotion of the production of inflammatory factors and infiltration of immune cells, as well as regulation of fibrosis-related gene expression, thereby contributing to the development of renal lesions<sup>37–39</sup>. In general, reducing PI3K/AKT/mTOR signaling could serve as a therapeutic approach to mitigate podocyte injury in DN<sup>38</sup>. In this study, RT-qPCR analysis demonstrated that fermented seaweed extracts inhibit the activation of the PI3K/Akt/mTOR pathway, suggesting a potential involvement of the PI3K/Akt pathway in the treatment with fermented seaweed extracts. Similarly, fermented astragalus and rutin have been shown to modulate the PI3K/AKT/mTOR signaling pathway in DN and induce autophagy in podocytes, thereby alleviating diabetic nephropathy<sup>7,39</sup>. Moreover, it has been demonstrated that alginate oligosaccharides alleviate cisplatin-induced kidney oxidative stress by inhibiting the Nrf2 pathway, thereby reducing oxidative stress in the kidneys of mice<sup>33</sup>. Additionally, luteolin has been reported to attenuate renal fibrosis in diabetic nephropathy by modulating the AMPK/NLRP3/TGF- $\beta$  signaling pathway<sup>40</sup>. Furthermore, short-chain fatty acids improve renal fibrosis in diabetic nephropathy through GPR43-mediated inhibition of oxidative stress and NF- $\kappa$ B signaling<sup>41</sup>. These pathways may also indirectly influence the PI3K/Akt/mTOR pathway. However, further research is necessary to clarify the specific downstream molecular mechanisms that underlie the effects of fermented seaweed extracts. Future studies should consider incorporating specific autophagy markers, such as LC3 and autophagy-related genes to validate the role of autophagy in the observed effects.

## Conclusion

Our data illustrated the protective role of fermented seaweed extracts in mitigating renal injury in diabetic nephropathy. The underlying mechanism may involve the inhibition of the PI3K/Akt/mTOR pathway (Fig. 6). These findings suggest that fermented seaweed extracts show potential for the development of functional foods and therapeutic strategies for diabetic nephropathy.

## Materials and methods

### Drugs and reagents

*Laminaria japonica* was purchased from Tulip Crown Foods Co., Ltd. (Fuzhou, China). Analytical grade  $\text{KH}_2\text{PO}_4$ ,  $\text{Na}_2\text{CO}_3$  and NaCl were obtained from Sinopharm Chemical Reagent Co (Shanghai, China). Acid cellulase, acid pectinase and alkaline pectinase was purchased from Shandong Nuojie Biotechnology Co (Weifang, China). Streptozotocin (STZ, 18883-66-4) were purchased from Shanghai McLean Biochemical Technology Co (Shanghai, China). Captopril tablets were purchased from Wuhan Xiangya Pharmaceutical Co (Wuhan, China). ELISA kits for serum creatinine (SCr, JM-10435R1), serum urea nitrogen (BUN, JM-10436R1), serum insulin (FINS, JM-01993R1), and urinary microalbumin (m-ALB, JM-10812R1) were purchased from Jiangsu Jingmei Biotech Co (Jiangsu, China). Antibodies including PI3K (A22457), P-PI3K (AF3242), AKT (A11016), P-AKT

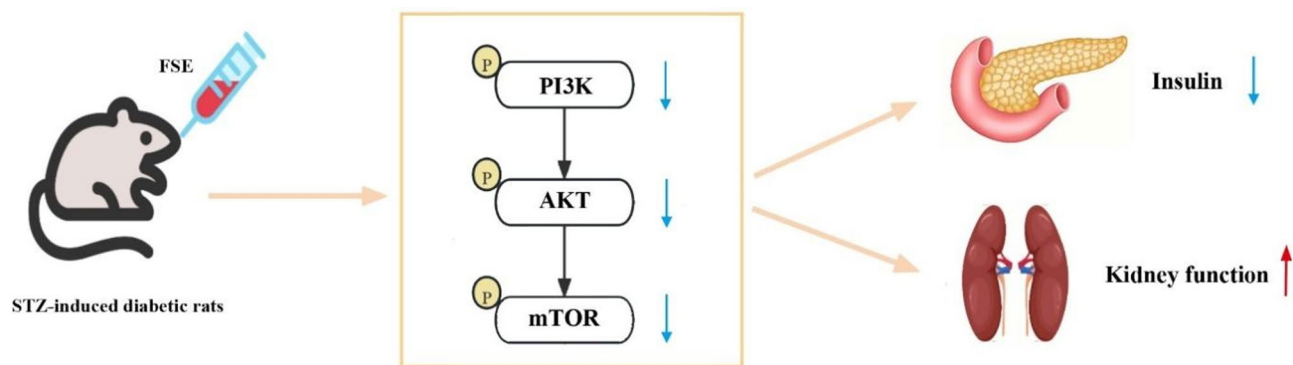


**Fig. 6.** The proposed mechanism of FSE in ameliorating diabetic nephropathy.

(AP0637), mTOR (A25581), P-mTOR (AP0490), and  $\beta$ -actin (AC026) were from ABclonal (China). P-PI3K (AF3242) were supplied by Affinity (USA).

### Strains and growth conditions

*Saccharomyces cerevisiae* (AMnb091), *Lactiplantibacillus plantarum* (LP1406), and *Lactiplantibacillus rhamnosus* (F-B4-1) were isolated in the laboratory, and assigned the culture preservation numbers CCTCC NO: M20211499, CCTCC NO: M20211500 and CCTCC M20221626, respectively. The yeast strain was cultured in YPD media at 30 °C with constant shaking at 180 rpm for 24 h, while the two *Lactiplantibacillus* strains were grown in MRS broth at 37 °C for 24 h before use.

### Preparation of fermented seaweed extracts

Fermented *Laminaria japonica* was prepared as described previously<sup>14</sup>. The seaweed was first washed, dried, ground, and sieved through a 40-mesh screen. The resulting powder underwent enzymatic hydrolysis using acidic and alkali enzymes. The reaction products were then sterilized and utilized as fermentation media. The fermentation process involved two steps: initial fermentation with *S. cerevisiae* followed by fermentation with *Lactiplantibacillus*. Specifically, a 3% (v/v) culture of *S. cerevisiae* was incubated at 30 °C for 48 h with agitation. The fermentation broth was then sterilized at 121 °C for 20 min before inoculating *L. plantarum* and *L. rhamnosus* at a 3% (v/v) concentration for an additional 48-hour incubation at 37 °C. The resulting Fermented *Laminaria japonica* was obtained through centrifugal separation and lyophilization. The lyophilized powder was subsequently extracted with aqueous ethanol (70%) at a 1:10 (w/v) ratio, stored at 4 °C overnight, and centrifuged to collect the supernatant for fermented seaweed extracts. This supernatant was lyophilized and stored at –20 °C for further analyses.

### Determination of chemical components in fermented seaweed extracts

Chemical components in fermented seaweed extracts were analyzed according to previous methods<sup>42</sup>. The samples were subjected to ashing in a muffle furnace (YTH-5-12 A, Shanghai Suoyu Test Equipment Co., Ltd., China) at a temperature of 550 °C for a duration of 5 h. The weight difference before and after ashing was used to calculate the sample losses. The carbohydrate content was determined using the phenol-sulphuric acid method in conjunction with a UV-visible spectrophotometer (Hitachi U 2910)<sup>43</sup>. Protein concentration was quantified using the Bradford method<sup>44</sup>. Total titratable acidity was assessed in accordance with the International Organisation for Standardisation (ISO) 750:1998. The soluble dietary fiber content was analyzed by the enzyme-weight method (AOAC 991.43). Total phenol content was measured using the Folin-Ciocalteu method<sup>45</sup>. The fat content was evaluated following the standard method (AOAC 996.06). Finally, free amino acid content was determined using the ninhydrin colorimetric method.

### Ultra high pressure liquid chromatography/tandem mass spectrometry (UHPLC-MS/MS) analysis

Fermented seaweed extract samples (500  $\mu$ L) were filtered through a 0.22  $\mu$ m membrane and then analyzed using ultra-high performance liquid chromatography-tandem mass spectrometry (UHPLC-MS/MS). The analysis was conducted on a Waters ACQUITY UHPLC system (H-Class, USA) coupled with a Bruker Q-TOF-MS mass spectrometer (Impact II, Germany). Liquid chromatography was carried out on an Agilent RRHD SB-C18 column (2.1  $\times$  100 mm, 1.8  $\mu$ m) with acetonitrile (solvent A) and water with 0.1% formic acid (solvent B). The gradient elution method started at 2% A and reached 98% B at 20 min. Injection volume was 3  $\mu$ L for both compound and standard samples. Data were acquired in positive and negative ion modes using the following ESI parameters: capillary voltage of 3500 V (positive) and 3000 V (negative), dry gas flow rate of 8 L/min, nebulizer pressure of 2.0 Bar, and drying temperature of 220 °C. Mass scanning was performed in the range of 50–1500 with retention time correction, peak identification, and alignment conducted using Compass Data Analysis 4.4 software. Compound identification was based on peaks with MSMS data matched against the Mass Bank mass spectrometry database.

Gene	Sequences	
PI3K	Forward (5'-3')	TTA AAC GCG AAG GCA ACGA
	Reverse (5'-3')	CAG TCT CCT CCT GCT GTC GAT
Akt	Forward (5'-3')	GGA CAA CCG CCA TCC AGA CT
	Reverse (5'-3')	GCC AGG GAC ACC TCC ATC TC
mTOR	Forward (5'-3')	GTG TGG CAA GAG CGG CAG AC
	Reverse (5'-3')	TGT TGG CAG AGG ATG GTC AAG TTG
β-actin	Forward (5'-3')	GCA GTT GGT TGG AGC AA
	Reverse (5'-3')	ATG CCG TGG ATA CTT GGA

**Table 3.** Primers sequences of RT-qPCR.

### Animal experimental design

Five-week-old male Wistar rats weighing 200–220 g were obtained from Beijing Viton Lihua Laboratory Animal Technology Co. The rats were provided with ad libitum access to food and water. Following a one-week acclimatization period, the rats were intraperitoneally injected with STZ (50 mg/kg) after a 12-hour fast<sup>46</sup>. STZ was dissolved in ice-cold citrate buffer (0.1 M, pH 4.5). Fasting blood glucose levels were measured 48 hours post-STZ injection, and rats exhibiting fasting blood glucose levels exceeding 16.7 mM for three consecutive days, accompanied by polyuria, were classified as diabetic and included in the study. Following successful modeling, the diabetic rats were randomly assigned to four groups: the model group (DN), the positive control group receiving captopril (10 mg/kg)<sup>47</sup>, and two groups receiving different doses of FSE (0.4, 0.8 g/kg)<sup>48</sup>, with 6 rats in each group. FSE and captopril were dissolved in saline at the specified dosage, with both the model group and the blank group (NC) receiving an equivalent amount of normal saline. The treatment period lasted for 14 weeks. The body weights of the rats were recorded weekly. After 14 weeks of administration, urine was collected from the rats using a metabolic cage. The urine was then centrifuged at 4 °C at 8000 rpm for 15 min, and the resulting supernatant was used for biochemical assays. Following this, blood was collected from the orbital vein under anesthesia with tribromoethanol (0.2 g/kg), and then the rats were sacrificed by cervical dislocation. The serum was centrifuged at 10,000 rpm for 10 min and stored at -80 °C for analysis. Kidneys were collected from rats in each group and weighed. The renal index was calculated as follows: renal index = kidney weight (g)/body weight (g) × 100%<sup>41</sup>.

The experimental procedures were performed under ARRIVE guidelines for the Care and Use of Laboratory Animals and approved by the Animal Ethics Committee of Qilu University of Technology (Shandong Academy of Sciences) (No. SWS20230303). All experiments were performed in accordance with relevant guidelines and regulations.

### Measurement of metabolic and biochemical parameters

The fasting blood glucose (FBG) levels of rats were monitored weekly throughout the experiment, with fasting insulin (FINS) levels assessed in the final week using an Elisa kit (JM-01993R1; Jingmei, Jiangsu, China). The homeostasis model assessment of insulin resistance (HOMA-IR) was calculated using the formula: HOMA-IR = (FINS × FBG)/22.5<sup>49</sup>. Urine samples underwent centrifugation, and supernatants were collected for the measurement of urinary microalbuminuria (mALB). Serum creatinine (SCr) and serum urea nitrogen (BUN) levels were determined following manufacturer protocols.

### Pathological examination of kidney tissue

Kidney tissues were cut into small pieces, fixed in 4% paraformaldehyde for 24 h, embedded in paraffin, sectioned at a thickness of 4 μm, and then stained with Hematoxylin and Eosin (H&E) as well as Periodic Acid Schiff (PAS) using the respective staining kits from Solarbio Technology Co., Ltd., Beijing, China. Subsequently, observations and photography were conducted using a light microscope (NIKON ECLIPSE E200, Nikon, Japan) at a magnification of 400X. The severity of kidney injury was assessed semiquantitatively in accordance with established literature<sup>50,51</sup>. The quantification of PAS-positive areas was conducted following the methodologies described in the literature<sup>52</sup>.

### Quantitative real-time PCR (RT-qPCR)

Total RNA was isolated from kidney tissue using TRIzol (Thermo Fisher Scientific) reagent and subjected to real-time fluorescence quantitative PCR. The RNA was reverse transcribed to cDNA using the Rapid One-Step cDNA Synthesis Kit (ABclonal Technology Co., Ltd.). RT-PCR was performed using SYBR green fluorescent fuel following the manufacturer's instructions. Amplification was carried out using a three-step real-time fluorescence quantitative PCR system. Gene expression of PI3K, Akt, and mTOR was normalized to GAPDH, and calculated using the  $2^{-\Delta\Delta Ct}$  method<sup>15</sup>. The rat primer sequences are shown in Table 3.

### Western blot (WB) analysis

Homogenize total protein from the kidney cortex in RIPA lysis buffer (Beyotime, China). The lysates were centrifuged at 4 °C at 12,000 ×g for 5 min, and the supernatant was collected, repeating this process three times. Protein concentrations were measured using the BCA Protein Assay Kit (Beyotime, China). An equivalent amount of protein was separated by 8% or 12% SDS-PAGE and subsequently transferred to a PVDF membrane.

The membrane was blocked with 5% BSA for 1 h, after which antibodies against Akt (1:2000), p-Akt (1:1000), mTOR (1:2000), p-mTOR (1:2000), PI3K (1:2000), p-PI3K (1:1000), and  $\beta$ -Actin (1:5000) were added and incubated overnight at 4 °C. After washing with 1 × TBST, the membrane was incubated with the corresponding secondary antibody (1:10000) for 1 h at room temperature. The target protein bands were then detected using an ECL kit (Seven, China), and these bands were quantified using ImageJ 1.8.0.

### Statistical analysis

All numerical values in the text are reported as mean  $\pm$  standard deviation. Statistical analysis was performed using GraphPad Prism 8.0.1, with group differences evaluated using one-way analysis of variance (ANOVA) and Tukey multiple-comparison test. A p-value less than 0.05 was considered statistically significant. GraphPad Prism 8.0.1, and Adobe Photoshop 2021 were utilized for creating images.

### Data availability

All data analysed during this study are included in this article and supplementary materials.

Received: 15 September 2024; Accepted: 11 June 2025

Published online: 02 July 2025

### References

1. Umanath, K. & Lewis, J. B. Update on diabetic nephropathy: core curriculum 2018. *Am. J. Kidney Dis.* **71**(6), 884–895. <https://doi.org/10.1053/j.ajkd.2017.10.026> (2018).
2. Brownlee, M. The pathobiology of diabetic complications: a unifying mechanism. *Diabetes* **54**(6), 1615–1625. <https://doi.org/10.2337/diabetes.54.6.1615> (2005).
3. Giacco, F., Brownlee, M. & Schmidt, A. M. Oxidative stress and diabetic complications. *Circ. Res.* **107**(9), 1058–1070. <https://doi.org/10.1161/circresaha.110.223545> (2010).
4. Lim, A. Diabetic nephropathy - complications and treatment. *Int. J. Nephrol. Renovasc. Dis.* **7**, 361–381. <https://doi.org/10.2147/ijn.rd.S40172> (2014).
5. Fitton, J. H., Stringer, D. N. & Karpiniec, S. S. Therapies from fucoidan: an update. *Mar. Drugs*. **13**(9), 5920–5946. <https://doi.org/10.3390/md13095920> (2015).
6. Xue, R. et al. Mechanistic insight and management of diabetic nephropathy: recent progress and future perspective. *J. Diabetes Res.* **2017**(7). <https://doi.org/10.1155/2017/1839809.1839809> (2017).
7. Zhang, Y. et al. Elabela protects against podocyte injury in mice with streptozocin-induced diabetes by associating with the PI3K/Akt/mTOR pathway. *Peptides* **114**, 29–37. <https://doi.org/10.1016/j.peptides.2019.04.005> (2019b).
8. Yu, L., Wei, J. & Liu, P. Attacking the PI3K/Akt/mTOR signaling pathway for targeted therapeutic treatment in human cancer. *SEMIN CANCER BIOL.* **85**, 69–94. <https://doi.org/10.1016/j.semcancer.2021.06.019> (2021).
9. Vaishnudevi, D. & Viswanathan, P. Seaweed polysaccharides - new therapeutic insights against the inflammatory response in diabetic nephropathy. *Antiinflamm. Antiallergy Agents Med. Chem.* **15**(3), 178–190. <https://doi.org/10.2174/1871523016666170217104226> (2017).
10. Sørensen, L. E., Jeppesen, P. B. & Christiansen, C. B. Nordic seaweed and diabetes prevention: exploratory studies in KK-Ay mice. *Nutrients* **11**(6), null. <https://doi.org/10.3390/nu11061435> (2019).
11. Almutairi, M. G., Aldubayan, K. & Molla, H. Effect of seaweed (Ecklonia Cava extract) on blood glucose and insulin level on prediabetic patients: A double-blind randomized controlled trial. *Food Sci. Nutr.* **11**(2), 983–990. <https://doi.org/10.1002/fsn3.3133> (2023).
12. Bannon, C. D., Eckenberger, J. & Snelling, W. J. Low-Molecular-Weight Seaweed-Derived polysaccharides lead to increased faecal bulk but do not alter human gut health markers. *Foods* **10**(12). <https://doi.org/10.3390/foods10122988> (2021).
13. Hur, S. J., Lee, S. Y., Kim, Y. C., Choi, I. & Kim, G. B. Effect of fermentation on the antioxidant activity in plant-based foods. *Food Chem.* **160**, 346–356. <https://doi.org/10.1016/j.foodchem.2014.03.112> (2014).
14. Yue, Q. et al. Changes in metabolite profiles and antioxidant and hypoglycemic activities of Laminaria Japonica after fermentation. *LWT* **158**, 113122. <https://doi.org/10.1016/j.lwt.2022.113122> (2022).
15. Mohammed, M. E. et al. Effect of Acacia senegal on TGF- $\beta$ 1 and vascular mediators in a rat model of diabetic nephropathy. *Arch. Physiol. Biochem.* **128**(6), 1548–1558. <https://doi.org/10.1080/13813455.2020.1781901> (2022).
16. Zhang, P. et al. Long non-coding RNA Rpph1 promotes inflammation and proliferation of mesangial cells in diabetic nephropathy via an interaction with Gal-3. *Cell. Death Dis.* **10**(7), 526. <https://doi.org/10.1038/s41419-019-1765-0> (2019a).
17. Yang, C. F. et al. Anti-diabetic effect of oligosaccharides from seaweed Sargassum confusum via JNK-IRS1/PI3K signalling pathways and regulation of gut microbiota. *Food Chem. Toxicol.* **131**, 110562. <https://doi.org/10.1016/j.fct.2019.110562> (2019).
18. Kim, Y. J., Kim, Y. A. & Yokozawa, T. Protection against oxidative stress, inflammation, and apoptosis of high-glucose-exposed proximal tubular epithelial cells by Astaxanthin. *J. Agric. Food Chem.* **57**(19), 8793–8797. <https://doi.org/10.1021/jf9019745> (2009).
19. Magee, C., Grieve, D. J., Watson, C. J. & Brazil, D. P. Diabetic nephropathy: a tangled web to unweave. *Cardiovasc. Drugs Ther.* **31**(5–6), 579–592. <https://doi.org/10.1007/s10557-017-6755-9> (2017).
20. Huang, W. et al. Short-chain fatty acids ameliorate diabetic nephropathy via GPR43-mediated Inhibition of oxidative stress and NF- $\kappa$ B signaling. *Oxid. Med. Cell. Longev.* **2020**, 4074832. <https://doi.org/10.1155/2020/4074832> (2020).
21. Zhou, T. et al. Sodium butyrate attenuates diabetic kidney disease partially via histone butyrylation modification. *Mediators Inflamm.* **2022**, 7643322. <https://doi.org/10.1155/2022/7643322> (2022).
22. Wang, L. et al. Two ascophyllum nodosum fucoidans with different molecular weights inhibit inflammation via blocking of TLR/NF- $\kappa$ B signaling pathway discriminately. *Foods* **11**(15). <https://doi.org/10.3390/foods11152381> (2022).
23. Xu, J., Wang, Y., Wang, Z., Guo, L. & Li, X. Fucoidan mitigated diabetic nephropathy through the downregulation of PKC and modulation of NF- $\kappa$ B signaling pathway: in vitro and in vivo investigations. *Phytother. Res.* **35**(4), 2133–2144. <https://doi.org/10.1002/ptr.6966> (2021).
24. Agarwal, S., Singh, V. & Chauhan, K. Antidiabetic potential of seaweed and their bioactive compounds: a review of developments in last decade. *Crit. Rev. Food Sci. Nutr.* **63**(22), 5739–5770. <https://doi.org/10.1080/10408398.2021.2024130> (2023).
25. Costa, L. S. et al. Antioxidant and antiproliferative activities of heterofucans from the seaweed Sargassum filipendula. *Mar. Drugs*. **9**(6), 952–966. <https://doi.org/10.3390/md9060952> (2011).
26. Wu, S. et al. Ethanol extract of sargassum fusiforme alleviates HFD/STZ-induced hyperglycemia in association with modulation of gut microbiota and intestinal metabolites in type 2 diabetic mice. *Food Res. Int.* **147**, 110550. <https://doi.org/10.1016/j.foodres.2021.110550> (2021).
27. Dai, H., Liu, Q. & Liu, B. Research progress on mechanism of podocyte depletion in diabetic nephropathy. *J. Diabetes Res.* **2017**, 2615286. <https://doi.org/10.1155/2017/2615286> (2017).

28. Fan, X., Li, Z., Wang, X., Wang, J. & Hao, Z. Silencing of KPNA2 inhibits high glucose-induced podocyte injury via inactivation of mTORC1/p70S6K signaling pathway. *Biochem. Biophys. Res. Commun.* **521**(4), 1017–1023. <https://doi.org/10.1016/j.bbrc.2019.10.200> (2020).
29. Lu, Q. et al. Clinical efficacy of Jinshuibao capsules combined with angiotensin receptor blockers in patients with early diabetic nephropathy: a Meta-Analysis of randomized controlled trials. *Evid. Based Complement Alternat. Med.* **2018**, 6806943. <https://doi.org/10.1155/2018/6806943> (2018).
30. Xu, J. et al. Effects of bailing capsule on diabetic nephropathy based on UPLC-MS urine metabolomics. *RSC Adv.* **9**(62), 35969–35975. <https://doi.org/10.1039/c9ra05046a> (2019).
31. Yang, F. et al. Paecilomyces cicadae-fermented Radix astragali activates podocyte autophagy by attenuating PI3K/AKT/mTOR pathways to protect against diabetic nephropathy in mice. *Biomed. Pharmacother.* **129**, 110479. <https://doi.org/10.1016/j.biopha.2020.110479> (2020).
32. Wang, Y., Li, L., Ye, C., Yuan, J. & Qin, S. Alginate oligosaccharide improves lipid metabolism and inflammation by modulating gut microbiota in high-fat diet fed mice. *Appl. Microbiol. Biotechnol.* **104**(8), 3541–3554. <https://doi.org/10.1007/s00253-020-10449-7> (2020).
33. Zhang, Y., Zhang, Y., Qin, S., Qin, S. & Song, Y. Alginate oligosaccharide alleviated cisplatin-induced kidney oxidative stress genus-FAHFs-Nrf2 axis in mice. *Front. Immunol.* **13**, 857242. <https://doi.org/10.3389/fimmu.2022.857242> (2022).
34. Huang, W. Short-chain fatty acids ameliorate diabetic nephropathy via GPR43-mediated Inhibition of oxidative stress and NF- $\kappa$ B signaling. *Oxid. Med. Cell. Longev.* **4074832** <https://doi.org/10.1155/2020/4074832> (2020).
35. Inoki, K., Li, Y., Zhu, T., Wu, J. & Guan, K. L. TSC2 is phosphorylated and inhibited by Akt and suppresses mTOR signalling. *Nat. Cell. Biol.* **4**(9), 648–657. <https://doi.org/10.1038/ncb839> (2002).
36. Huang, R. et al. Luteolin Alleviates Diabetic Nephropathy Fibrosis Involving AMPK/NLRP3/TGF- $\beta$  Pathway. *Diabetes Metab. Syndr. Obes.* **30**, 17:2855–2867. <https://doi.org/10.2147/DMSO.S450094>. (2024).
37. Rinne, N., Christie, E. L., Ardasheva, A., Kwok, C. H. & Demchenko, N. Targeting the PI3K/AKT/mTOR pathway in epithelial ovarian cancer, therapeutic treatment options for platinum-resistant ovarian cancer. *CANCER DRUG RESIST.* **4**(3), 573–595. <https://doi.org/10.20517/cdr.2021.05> (2021).
38. Dong, R. et al. Rutin alleviates EndMT by restoring autophagy through inhibiting HDAC1 via PI3K/AKT/mTOR pathway in diabetic kidney disease. *Phytomedicine* **112**, 154700. <https://doi.org/10.1016/j.phymed.2023.154700> (2023).
39. Yu, Q., Zhang, M., Qian, L., Wen, D. & Wu, G. Luteolin attenuates high glucose-induced podocyte injury via suppressing NLRP3 inflammasome pathway. *Life Sci.* **225**, 1–7. <https://doi.org/10.1016/j.lfs.2019.03.073> (2019).
40. Ural, C., Celik, A., Ozbal, S., Guneli, E. & Guneli, E. The renoprotective effects of taurine against diabetic nephropathy via the p38 MAPK and TGF- $\beta$ /Smad2/3 signaling pathways. *Amino Acids.* **55**(11), 1665–1677. <https://doi.org/10.1007/s00726-023-03342-w> (2023).
41. Xu, H. L. et al. Ursolic acid improves diabetic nephropathy via suppression of oxidative stress and inflammation in streptozotocin-induced rats. *Biomed. Pharmacother.* **105**, 915–921. <https://doi.org/10.1016/j.biopha.2018.06.055> (2018).
42. Yue, Q., Wang, Z. & Tang, X. Hypolipidemic effects of fermented seaweed extracts by saccharomyces cerevisiae and Lactiplantibacillus plantarum. *Front. Microbiol.* **12**, 772585. <https://doi.org/10.1155/jfbc/1706266> (2021).
43. Wang, D. et al. Antioxidative and hepatoprotective effects of the polysaccharides from Zizyphus jujube Cv. Shaanbeitanzao Carbohydr. Polym. **88**(4), 1453–1459. <https://doi.org/10.1016/j.carbpol.2012.02.046> (2012).
44. Bradford, M. M. & Rapid, A. and Sensitive method for the quantitation of microgram quantities of protein utilizing the principle of protein-dye binding. *Anal. Biochem.* **72**, 248–254. [https://doi.org/10.1016/0003-2697\(76\)90527-3](https://doi.org/10.1016/0003-2697(76)90527-3), 2-s2.0-0017184389. (1976).
45. McDonald, S., Prenzler, P. D., Antolovich, M. & Robards, K. Phenolic content and antioxidant activity of olive extracts. *Food Chem.* **73**(00)00288-0, 73–84. <https://doi.org/10.1016/s0308-8146> (2001).
46. Hang, Q., Ji, Y., Lv, W., He, T. & Wang, J. Protective effects of Leflunomide on renal lesions in a rat model of diabetic nephropathy. *Ren. Fail.* **38**(1), 124–130. <https://doi.org/10.3109/0886022X.2015.1105024> (2015).
47. Xu, Y., Zhang, Q., Luo, D., Wang, J. & Duan, D. Low molecular weight fucoidan modulates P-selectin and alleviates diabetic nephropathy. *Int. J. Biol. Macromol.* **91**, 233–240. <https://doi.org/10.1016/j.ijbiomac.2016.05.081> (2016).
48. Yue, Q. et al. Hypolipidemic effects of fermented seaweed extracts by Saccharomyces cerevisiae and Lactiplantibacillus plantarum. *Front. Microbiol.* **12**, 772585. <https://doi.org/10.3389/fmicb.2021.772585> (2021).
49. Matthews, D. R. et al. Homeostasis model assessment: insulin resistance and beta-cell function from fasting plasma glucose and insulin concentrations in man. *Diabetologia* **28**(7), 412–419. <https://doi.org/10.1007/bf00280883> (1985).
50. Tomkins, M., Lawless, S., Martin-Grace, J., Sherlock, M. & Thompson, C. J. Diagnosis and management of central diabetes insipidus in adults. *J. Clin. Endocrinol.* **90**(1), 23–30. <https://doi.org/10.1111/cen.13866> (2022).
51. Patti, G., Patti, G., Napoli, F., Fava, D. & Fava, D. Approach to the pediatric patient: central diabetes insipidus. *J. Clin. Endocrinol. Metab.* **107**(5), 1407–1416. <https://doi.org/10.1210/clinem/dgab930> (2022).
52. Li, X. Z., Jiang, H., Xu, L., Liu, Y. Q. & Tang, J. W. Sarsasapogenin restores podocyte autophagy in diabetic nephropathy by targeting GSK3 $\beta$  signaling pathway. *Biochem. Pharmacol.* **192**, 114675. <https://doi.org/10.1016/j.bcp.2021.114675> (2021).

## Author contributions

M. C.: Investigation, formal analysis, data curation and writing-original draft. G. H.: Investigation, formal analysis, data curation and writing-original draft. S. G.: Investigation and formal analysis. Y. L.: Investigation and formal analysis. C. Z.: Investigation and formal analysis. L. Z.: Formal analysis and methodology. L. S.: Methodology. K. L.: Data curation. Q. Y.: Conceptualization, writing-reviewing, editing, and funding acquisition. S. Z.: Project administration and funding acquisition.

## Funding

This work was supported by the Key Technology Research and Development Program of Shandong Province (Competitive provincial innovation platform project) [grant number 2023CXPT037]; the Central Government Guides Local Science and Technology Development Special Fund Project [grant number YDZX2021051]; Innovation capability improvement project for SMEs of Shandong Province [grant number 2022TSGC1076]; the Scientific and Technological Project in Jinan [grant number 202131004]; and the XGCC Financial Science and Technology Project in 2022 [grant number 2022AB002].

## Declarations

## Competing interests

The authors declare no competing interests.

### Additional information

**Supplementary Information** The online version contains supplementary material available at <https://doi.org/10.1038/s41598-025-06935-5>.

**Correspondence** and requests for materials should be addressed to Q.Y. or S.Z.

**Reprints and permissions information** is available at [www.nature.com/reprints](http://www.nature.com/reprints).

**Publisher's note** Springer Nature remains neutral with regard to jurisdictional claims in published maps and institutional affiliations.

**Open Access** This article is licensed under a Creative Commons Attribution-NonCommercial-NoDerivatives 4.0 International License, which permits any non-commercial use, sharing, distribution and reproduction in any medium or format, as long as you give appropriate credit to the original author(s) and the source, provide a link to the Creative Commons licence, and indicate if you modified the licensed material. You do not have permission under this licence to share adapted material derived from this article or parts of it. The images or other third party material in this article are included in the article's Creative Commons licence, unless indicated otherwise in a credit line to the material. If material is not included in the article's Creative Commons licence and your intended use is not permitted by statutory regulation or exceeds the permitted use, you will need to obtain permission directly from the copyright holder. To view a copy of this licence, visit <http://creativecommons.org/licenses/by-nc-nd/4.0/>.

© The Author(s) 2025